THE UNIVERSITY of EDINBURGH

Edinburgh Research Explorer

Modelling, Control and Frequency Domain Analysis of a Tidal Current Conversion System with Onshore Converters

Citation for published version:
Sousounis, M, Shek, J & Mueller, M 2015, 'Modelling, Control and Frequency Domain Analysis of a Tidal Current Conversion System with Onshore Converters', *IET Renewable Power Generation*. https://doi.org/10.1049/iet-rpg.2014.0331

Digital Object Identifier (DOI):
10.1049/iet-rpg.2014.0331

Link:
Link to publication record in Edinburgh Research Explorer

Document Version:
Early version, also known as pre-print

Published In:
IET Renewable Power Generation

General rights
Copyright for the publications made accessible via the Edinburgh Research Explorer is retained by the author(s) and / or other copyright owners and it is a condition of accessing these publications that users recognise and abide by the legal requirements associated with these rights.

Take down policy
The University of Edinburgh has made every reasonable effort to ensure that Edinburgh Research Explorer content complies with UK legislation. If you believe that the public display of this file breaches copyright please contact openaccess@ed.ac.uk providing details, and we will remove access to the work immediately and investigate your claim.

Download date: 07. May. 2023

Modelling, Control and Frequency Domain Analysis of a Tidal Current Conversion System with Onshore Converters

Marios C. Sousounis, Jonathan K. H. Shek, Markus A. Mueller

Institute for Energy Systems, School of Engineering, The University of Edinburgh, The King's Buildings, Mayfield Road, Edinburgh, EH9 3JL, United Kingdom

Email: M.Sousounis@ed.ac.uk

Abstract

In order to optimise a tidal energy conversion system, the operation, maintenance and power generation aspects have to be taken into account. As a result the key focus of this paper is to propose and investigate an alternative method of implementing a tidal energy conversion system using a pitch-regulated turbine and a variable-speed squirrel cage induction generator with long distance converters. The generator power output can be optimised by utilising variable-speed control strategies allowing the system to operate at maximum power coefficient while availability can be increased by reducing the components installed offshore by using long three-phase cables between the generator and onshore voltage source converters. The tidal current energy conversion system is investigated by developing a full resource-to-grid model in MATLAB/Simulink and by performing system analysis regarding the effects of harmonics in the long subsea cables. Simulation results show that optimised filter design and the choice of suitable operating frequency for the generator controller can minimise the over-voltages associated with the harmonics and the reflecting voltage waves in the cables.

1 Introduction

The potential to generate low or zero carbon-free power from the world's tides is increasing as technology moves forward. The technically available tidal current energy resource, the resource that can be captured using existing technology, in the United Kingdom is significant and can supply 29% of the UK electricity demand based on 2013 statistics [1, 2]. At certain locations tidal currents can possess very high energy density which can

lead to large amounts of power. As a result of high energy density, devices are subjected to large forces in order to maximise conversion of the available energy but are still expected to operate reliably under harsh conditions. Even though they have similarities to offshore wind turbines in many aspects, a number of characteristics differentiate the approach needed regarding power transmission and drive-train design. Some of these characteristics are: predictable direction and speed of the tidal current, predetermined available area in a tidal channel, less swept area due higher density of water, continuous underwater operation and smaller distances to shore [3].

To be more specific, the continuous underwater operation requires that the tidal system must work reliably with high availability. This dictates that onsite visits must be reduced to a minimum since tidal devices are usually installed at locations with strong tidal currents. At these locations, the windows of opportunity for onsite visits are relatively short, which means that major operations need to be extremely quick or be able to continue in high flow speeds [3]. Another aspect of tidal arrays that affect power transmission is that they will be close enough to shore and therefore offshore substations and high-voltage subsea transmission can be avoided. Reducing the number of components installed offshore can consequently reduce offshore maintenance. In this context, it has been suggested that tidal energy developers can extend the availability of their systems by moving the power electronics from the nacelle to the shore. This could help to minimise onsite visits since the failure frequency of power converters can be significant based on data from onshore wind turbines [4]. Locating the power electronics on land means that the generator has to be controlled using long subsea cables and therefore long distance drives are needed. Long distance converters have been used to drive electrical submersible pumps in oil offshore platforms.

The literature regarding long distance drives focuses on the variable speed operation of low power motors [5]-[9] which are usually designed to be used as pumps in offshore oil platforms [7]-[9]. The main points discussed are the reasons behind the appearance of over-voltages at the terminals of motors with long feeders [5] [7], filtering techniques in order to mitigate the problems associated with the long feeders [5][6], and the importance of accurate frequency domain analysis in order to investigate system resonant frequency in different topologies [8]. In [10] authors investigate the appearance of overvoltages and resonant frequencies in a system with a medium voltage motor used as fan in an underground mine. They highlight the importance of a low voltage low pass filter installed at the inverter terminals by experimenting with and without filters and clearly showing the appearance of overvoltages at the motor terminals. In [6] authors also discuss the effect of long cables in a PWM vector controller of a low power induction motor.

Currently, tidal current turbine developers have not yet decided on the optimal tidal current conversion system (TCCS) and therefore a number of different designs exist. While most of the designs are bottom mounted with low solidity blades and horizontal axis rotors, the approaches differ in generator technology. Dominant choices are direct drive generators or geared permanent magnet synchronous generators (PMSGs) and squirrel cage induction generators (SCIGs). Power limitation is achieved using fixed pitch or variable pitch blades. Research papers regarding TCCS are focused on the mitigation of over-voltages in systems with long distance controls [11][12], the power limitation mechanisms [13][14], grid integration of tidal current conversion systems [15], power capture maximisation control methods and generator technologies [16][17].

Even though in [11] authors analyse a TCCS with long distance controls they assume a low power low voltage generator which can be installed at rivers or small tidal channels. At the moment the state of industry is to deploy small demonstration tidal arrays composed of up to 10 tidal turbines with 1MW capacity per turbine. For demonstration purposes and in order to achieve maximum availability tidal energy developers consider the separate connection to shore per turbine. However, this is only possible when the distance to shore is small, usually less than 10km and the number of installed devices limited.

A tidal array concept based on long distance controls is depicted in Figure 1a. In this tidal array concept each turbine is connected using three-phase subsea cables to the shore. In the nacelle, the gearbox, if the generator is not direct drive, the medium voltage (MV) generator and all the appropriate measurement and protection devices are installed. On the shore all the necessary electrical equipment is installed in order to control the tidal turbine, to step down the medium voltage (MV) to low voltage (LV) for a 2-level converter, to filter the harmonics and avoid cable resonance. After the active rectifier the power from all the turbines can be collected in the DC link and then transferred for grid connection using medium or high voltage DC transmission or using high voltage AC transmission (HVAC).

The aim of this paper is to present a full resource-to-grid dynamic model of a single tidal current turbine with the proposed long distance converters. A single tidal turbine is chosen since as it is depicted in Figure 1a, the tidal array concept with long distance controls is based on multiples of single devices with a common collection point. Even though the grid side is also modelled, the main focus of this paper is on the operation of the generator when the long distance controller is utilised. The system was first presented in [18] and is based on a three-bladed tidal turbine with pitch-regulated blades and a SCIG controlled using direct torque control with space vector modulation (DTC SVM). Utilising the dynamic model, we investigate the applicability of long distance converters in TCCS. In addition, we present the challenges associated with the use

of long subsea cables between the generator and the converter which include high harmonics and over-voltages at the cable ends due to resonance and voltage reflections. Section 2 briefly explains the modelling of the system. Section 3 shows the results from the simulation of the model and is separated in time domain and frequency domain simulations. In section 4 conclusions are drawn regarding the design of TCCS.

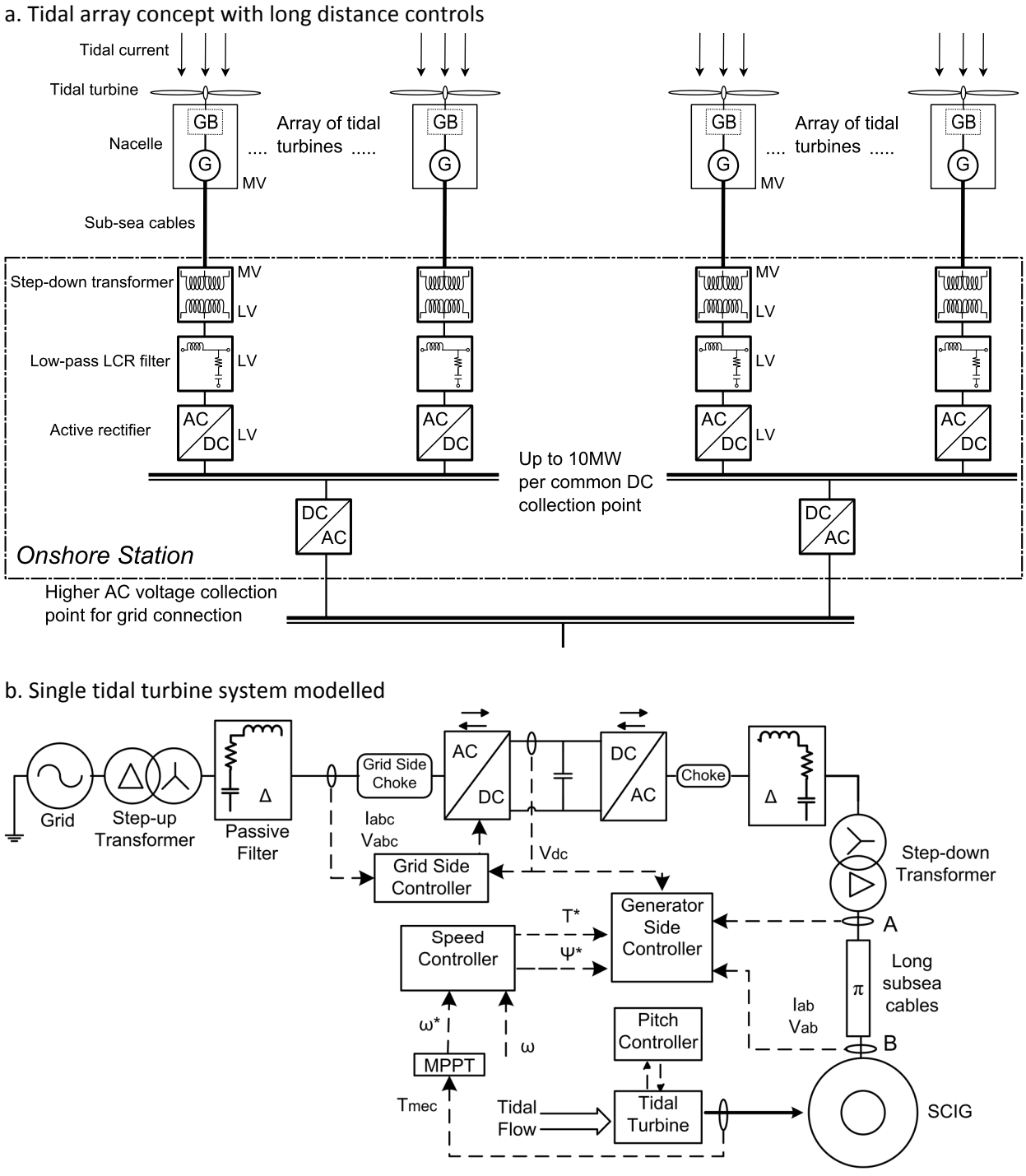

Figure 1. a. Tidal array concept **b.** The complete tidal current conversion system modelled

2 Modelling of tidal current conversion system

In this section all the modelling aspects of a TCCS will be described. The proposed topology can be seen in Figure 1b. The tidal turbine shaft is connected to the SCIG rotor through a gearbox. The output of the medium voltage generator (6.6kV) is transmitted to shore by long three-phase subsea cables. Cable modelling is described in detail in section 2.5. The medium voltage is transformed to low voltage (690V) using an onshore transformer. Generator and transformer parameters are given in the appendix. Between the voltage source converter (VSC) and the step-down transformer, filters are installed. The importance of appropriate filtering is discussed in section 2.6. In order to enable variable speed operation of the SCIG the generator side controller is implemented using the DTC SVM method which is discussed in section 2.4. On the grid side, the low voltage output of the inverter (690V) is first filtered and then a step-up transformer is used in order to match the high voltage at the grid (11kV). At the output of both VSCs, grid side and generator side, a choke is placed. The resistance and inductance of the choke in both cases is 0.05pu.

2.1 Tidal resource

The power potential of tidal currents can be derived by the same formula as for wind energy systems.

$$P_{tide} = 0.5 \times \rho_{water} \times A \times V_{current}^3 \qquad (1)$$

Where ρ_{water} is the sea water density approximately equal to 1025kgm^{-3}, A is the swept area considered and $V_{current}$ is the fluid speed in m/s.

For the purposes of this study the input flow speed is chosen to be a half-cycle with high peak flow as we intend to represent the most complex period of operation of the system. The flow speed is constructed by:

- The mean flow speed which is created based on actual tidal current measurements (Figure 2a).
- The predicted turbulence which is modelled by adding white noise.
- The swell effect of the tides by using a first-order Stokes model as described in [14] and [19]

The flow profile used as input to the model can be seen in Figure 2b.

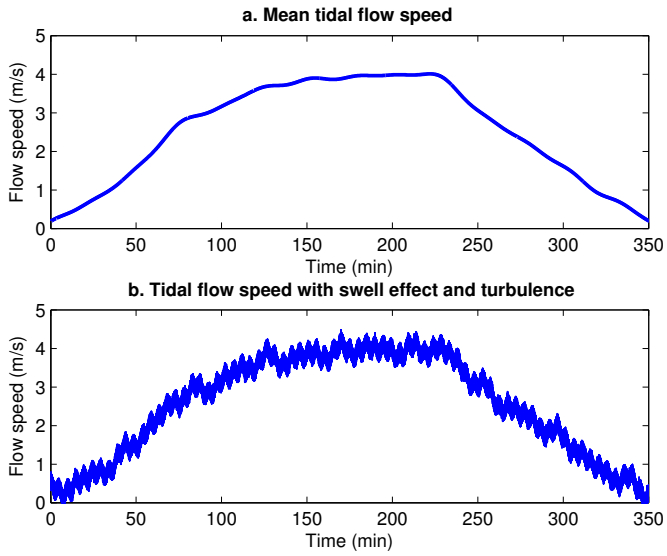

Figure 3. a. Mean tidal flow speed. **b.** Tidal flow speed used as input to the TCCS model.

2.2 Tidal turbine model

The model is based on the steady-state power characteristics of the turbine. The output power of the turbine is given by the following equation.

$$P_m = C_p(\lambda, \beta) \times P_{tide} \qquad (2)$$

Where P_m is the mechanical output power of the turbine in watts and $C_p(\lambda,\beta)$ is the power coefficient of the turbine which is a function of the tip speed ratio, λ, and blade pitch angle, β. In this model a maximum C_p of 0.48 is assumed and rated power is achieved at 2.5m/s [18].

2.3 Pitch controller

Power limitation in high tidal current speeds is achieved by using pitch angle control. This corresponds to changing the pitch value such that the leading edge of the blade is moved into the flow increasing the angle of attack and thus inducing a blade feathering effect. The control structure of the pitching system developed is published in [18]. The pitching mechanism limits the turbine speed to rated speed by reducing C_p in equation (2) and so reducing the mechanical power captured.

2.4 Generator Controller

In order to ensure variable speed operation the SCIG is controlled from an onshore VSC using DTC SVM. DTC SVM methods are based on the classical DTC [20] but they also operate at constant switching frequency. For the generator controller the DTC SVM scheme with closed-loop torque and flux control in stator flux

coordinates has been implemented [21]. The control structure of the DTC SVM method modelled can be seen in Figure 3.

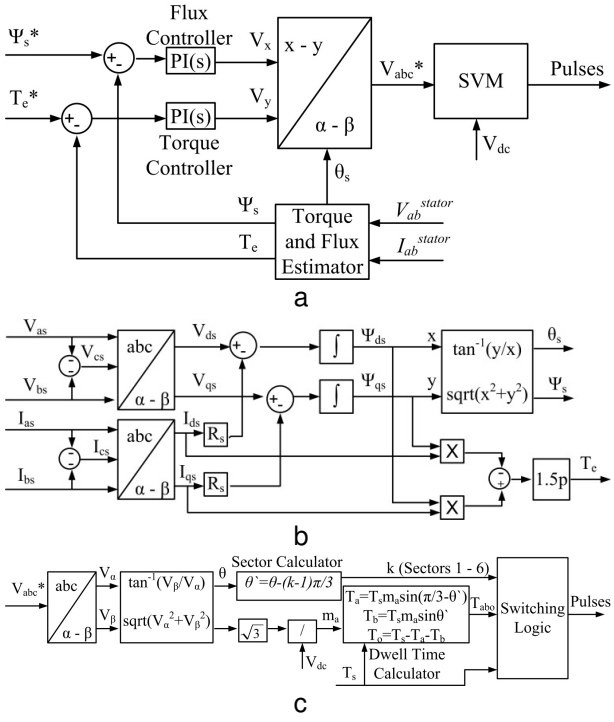

Figure 3. a. Block diagram of the DTC SVM method with closed-loop torque and flux control in stator flux coordinates. **b.** Block diagram of the torque and flux estimator. **c.** Block diagram of the space vector modulation method [22].

The DTC SVM method is composed of three distinct parts.

- The Torque and Flux Estimator.
- The Torque and Flux PI controllers
- The space vector modulation method

The torque and flux estimator calculates the actual stator flux and electrical torque of the generator by measuring the stator voltage and current. The block diagram of the estimator can be seen in Figure 3b. However, in a system with onshore converters the generator terminal, where the stator voltage and current of the generator can be measured (measuring point B in Figure 1b), is several kilometres away from the controller which is placed onshore. The time needed to transmit the measured quantities from offshore to onshore has to be less than or equal to the controller computation time. For the purposes of the simulation the controller computation time is equal to 200μs. Assuming a relatively high reduction of 66% of the speed of light in the fibre optics, the light in the fibre optics of the sub-sea cables can travel 0.1km/μs. For the marginal value of 200μs the maximum

cable length in which the information of measured quantities can reach the controller without delays is 20km. This means that in all the cases that long distance controls are considered in a TCCS the measurements can be taken from the generator terminals.

However, in many cases it is suggested that the measurements can be taken from an onshore point so that the transfer of information is easier. Therefore, it is possible to measure the voltage and current at the cable end (measuring point A in Figure 1b) and then estimate the stator voltage and current (voltage and current of point B) by knowing the cable parameters. The disadvantage of this method is that cable parameters change based on the operating frequency of the system and the temperature variations.

For this simulation study both measuring cases have been considered in order to identify deviations in results. Both cases produced similar or even identical results and for that reason the results presented in this paper are based on measurements from the generator terminals (measuring point B). At this point we need to note that cable variations where not considered when comparing the two different measuring cases.

2.5 Cable Modelling

The long subsea cables are modelled with a network of π-sections in order to accurately represent the uniform distribution of the cable resistance R_C, inductance L_C and capacitance C_C. The number of identical π-sections required to accurately represent frequency transients is given by the following equation:

$$N = \frac{8 \cdot l_C \cdot f_{\max}}{v_C} \quad (3)$$

Where v_C is the travelling speed of the waves in the cables and is defined in (4).

$$v_C = \frac{1}{\sqrt{L_C \cdot C_C}} \quad (4)$$

In this research paper the analysis is based on the particular cases in which ANDRITZ Hydro Hammerfest is involved. For the above reason a cable length of $3.5km$ has been chosen. Regarding the transient analysis of this system, this lies in the low frequency range and therefore $f_{max} = 5kHz$. The parameters of the cascaded π-network are given in Table 1. The cable model was based on the Pirelli cable used at the tidal site of EMEC and is described in [23]. The Pirelli cable is an $11kV$, three core ethylene propylene rubber (EPR) insulated submarine cable constructed for alternating current. It has an optical fibre unit, three $2.5mm^2$ copper signal cables and is double wire armoured.

Table 1 Submarine cable network parameters

Symbol	Quantity	Value
R_C	Cable resistance	0.197 Ω/km
L_C	Cable inductance	0.742 mH/km
C_C	Cable Capacitance	0.310 $\mu F/km$
$\lvert Z_C \rvert$	Cable characteristic impedance	52.5708 Ω
l_C	Cable length	3.5 km
N	Number of π-sections	2.12
$N`$	Number of π-sections chosen	3
$f_{max}`$	Maximum accurately represented frequency	7000 Hz

Since two π-sections cannot represent the frequency range of 5000Hz, we chose three π-sections that can actually represent $f_{max}`$.

2.6 Optimised filter design

The optimised passive filter for the generator side is based on a second-order *LCR (Low Voltage LCR)* filter for overvoltage mitigation which is described in detail for a converter-cable-generator system in [11], for a converter-cable-motor system in [6] and for a converter-transformer-cable-motor system in [10]. The system in this research paper is a converter-transformer-cable-generator system. In addition, the use of single tuned filter together with the *LV LCR* filter will be analysed. In this case the *LV LCR* filter is designed to reduce the overvoltage at the generator terminals and minimise the effects of resonance in the cables while at the same time the single tuned filter, tuned at the switching frequency of the controller, will mitigate the harmonics generated by the VSC that controls the generator. Figure 4 shows the generator side of the TCCS with the different options of filtering techniques.

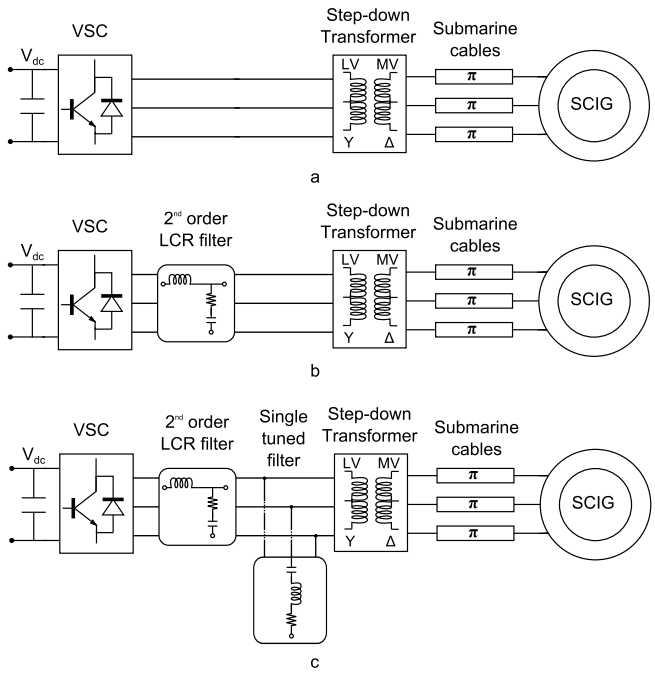

Figure 4. Block diagram of the generator side of the TCCS. a. System without filters b. System with a *LV LCR* filter c. System with a *LV LCR* filter and a single tuned filter.

The parameters of the *LV LCR* filter are given in Table 2 which are calculated using equations (5) – (7) which are described in detail in [6]. The actual difference in this research paper is that the transformer turns ratio has to be taken into account and therefore final filter parameters have to be referred to the primary winding of the transformer. More details regarding filter design equations for the *LV LCR* and the single tuned filter are given in [12].

$$R_{filter} = 2 \cdot \sqrt{\frac{L_{filter}}{C_{filter}}} = |Z_C| \qquad (5)$$

$$\sqrt{L_{filter} \cdot C_{filter}} \geq t_{critical} \qquad (6)$$

$$t_{critical} = 15 \cdot l_C \cdot \sqrt{L_C \cdot C_C} \qquad (7)$$

Table 2 *LV LCR* filter parameters

Symbol	Quantity	Value
R_{filter}	Filter resistance	0.1915 Ω
L_{filter}	Filter inductance	0.2728 mH
C_{filter}	Cable Capacitance	84.6701 μF

$t_{critical}$	Critical rise time	0.7962 *ms*

2.7 Grid side modelling

The power generated by the TCCS is delivered to the grid through a VSC. The grid-tied inverter is connected to the grid through a line reactor to reduce line current distortion, a filter that reduces harmonics and a step-up transformer from 690*V* to 11*kV* [18]. The inverter is controlled by a PWM scheme called voltage oriented control (VOC) with decoupled controllers [22] which ensures a constant DC link voltage of $1100V_{dc}$, constant frequency output of 50*Hz* on the AC side and control over the amount of reactive power flowing based on grid requirements.

3 Simulation results

3.1 Time domain simulation

In this section the operation of the proposed TCCS is demonstrated when a *LV LCR* filter is installed as described in Figure 4b. The necessity of using at least the *LV LCR* filter is explained by presenting the voltage waveform at the generator terminals when the TCCS is simulated with and without filters. Afterwards, simulation results are shown for the modelled TCCS operating for a half tidal cycle, which is about 350 minutes in this case.

In order to demonstrate the need of a generator side filter at the terminals of the VSC, the TCCS is modelled without filters, Figure 4a, and is simulated at a generator controller switching frequency of 2500*Hz*. The controller switching frequency of 2500*Hz* is compatible with the control loop computation time which is 200μs as described in section 2.4. The above means that the switching cycle takes 400μs while the control loop is refreshed twice during this time because the control loop computation time is half of the switching cycle time. In Figure 7a we can observe the voltage at the terminals of the generator without the filter. It can be seen that the maximum voltage is above 1.2pu of the rated voltage which is the acceptable limit when an over-voltage occurs. If the overvoltage is above the 1.2pu then there is a risk of insulation breakdown and system failure. Similar results have been presented in experimental research papers. In [6] authors presented the differences in motor and inverter voltage in a converter-cables-motor system. By showing this comparison it could be seen that overvoltages appeared at the motor terminals. This comparison was both simulation based and experimental and the overvoltages at the motor terminals were observed in both cases at similar magnitude. Another research study presented in [11] in a converter-transformer-cables-motor system compared simulated and experimental

voltage waveforms at the motor terminals without any filters. At this comparison it could be seen that simulation results are over-estimating the overvoltage at the generator terminals by approximately 0.25pu. This indicates that the actual performance of the system is better from the simulated in such a system but the overvotlages appearing are still outside acceptable limits. Based on these observations and the results presented in Figure 7a it is concluded that the TCCS under the proposed electrical configuration cannot operate without a filter to mitigate voltage reflections and system resonance.

Figure 7b depicts the voltage waveform at the generator terminals when the *LV LCR* filter is connected at the terminals of the VSC. The block diagram of this system is presented in Figure 4b. The peak generator voltage is 1.06pu which is well within the limits of 1.2pu. The reduction of voltage peaks, when a *LV LCR* filter is installed was expected based on experimental and simulation results presented in the literature for motors [6, 11].

Figure 5 shows the flow speed, the power generated by the SCIG, the pitch angle and the generator speed in a half tidal cycle simulation for the TCCS depicted in Figure 4b.

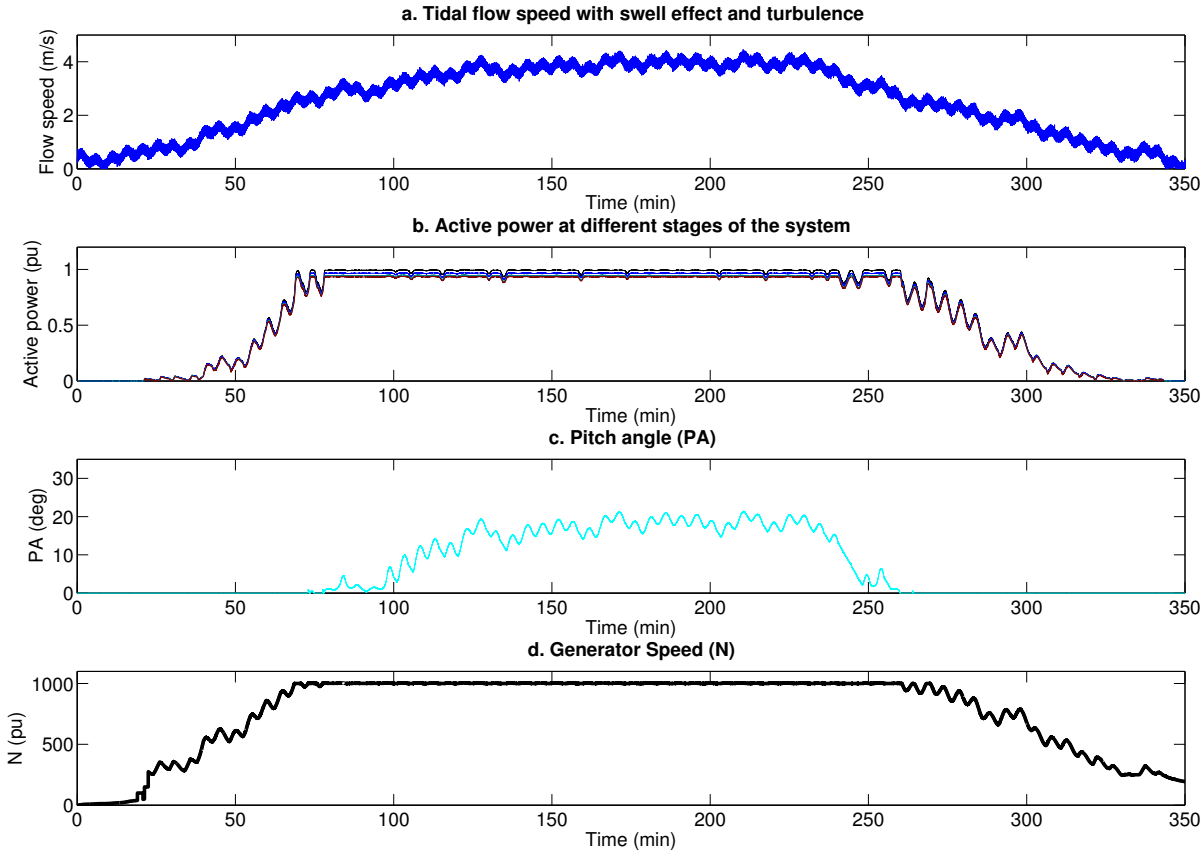

Figure 5. Flow speed, power generated, pitch angle and generator speed for a half tidal cycle of operation for the proposed TCCS with *LV LCR* filter.

3.2 Frequency-domain system analyses

In order to understand the ways the long cables affect the TCCS with long distance controls, the system should be analysed in the frequency domain. By doing so, system resonant frequencies can be identified in the frequency range of interest, and the effect these frequencies have on harmonics and how system response changes when a filter is added can be analysed.

In order to understand the magnitude of resonance voltage gain graphs were created. The voltage gain graph is produced by assuming that the VSC is sending voltage pulses and that the generator terminals are the receiving end of these pulses as described in [10]. Therefore we can compute the state-space model of the system using MATLAB. The voltage gain graph can be expressed as in equation (8).

$$V_{GAIN}(s) = \frac{V_{Gen}(s)}{V_{VSC}(s)} \qquad (8)$$

The V_{GAIN} graph reveals how the frequency components of the voltage pulses generated by the VSC are changing to reach the generator terminals. Specifically, if a frequency has a high value of V_{GAIN} then the harmonic components at this frequency will be magnified when they reach the generator terminals. On the other hand, if the V_{GAIN} has a small value at a specific frequency range then the harmonic components at these frequencies will be reduced at the generator terminals. The voltage gain graph also appears in the literature and is used by electrical companies mainly in the oil industry [24]. In [24] the voltage gain graph is presented as output-to-input voltage transmission ratio. Authors use this voltage ratio to determine the frequencies of the harmonics of the voltage output. In Figure 6 the voltage gain graphs of the generator side of the three TCCS presented in Figure 4 are depicted.

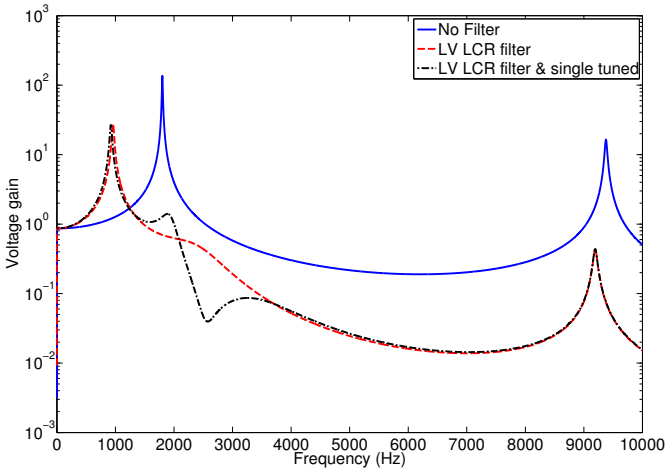

Figure 6. Voltage gain graphs of the TCCS proposed for the different filtering cases.

It is observed from Figure 6 that at some frequencies resonant peaks appear. In the first case, when no filters are installed, the resonant peaks appear at approximately 1800Hz and 9350Hz. In the second case, in which the *LV LCR* filter is installed, resonant peaks appear at approximately 800Hz and 9000Hz. Finally, in case 3, the same resonant peaks appear when a *LV LCR* filter and a single tuned filter are installed at the TCCS. Apart from the resonant peaks, at some frequencies resonant minimums appear as well. These minimums appear at approximately 6000Hz, 7000Hz and 2500Hz respectively for the three cases. The resonant minimum of 2500Hz in case 3 is created due to the filter tuned at 2500Hz.

From the above observations, it would be reasonable to test the effect of changing the controller switching frequency to values closer to the resonant minimum or away from the resonant maximum in order to achieve reduced harmonic distortion at the generator voltage.

3.2.1 The effect of the controller switching frequency on the harmonics of the generator voltage

In Figure 7 the voltage waveforms at the generator terminals for the three cases are depicted for different generator controller switching frequencies (f_{sw}). The generator controller switching frequencies chosen below are based on the resonant minimum presented in Figure 6. Additional results are presented at the end of the section in Table 3.

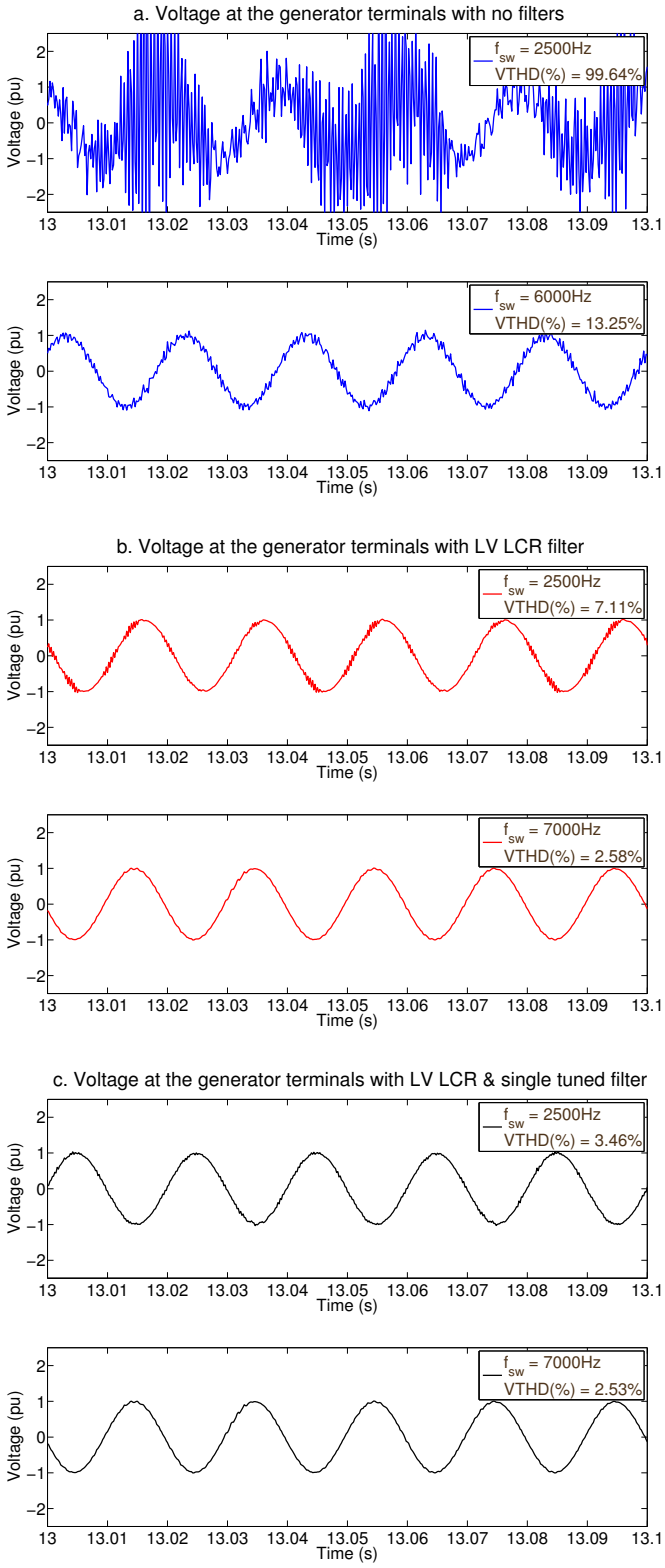

Figure 7. Comparison of voltage waveforms at the generator terminals for different generator controller switching frequencies a. No filter b. *LV LCR* filter c. *LV LCR* & single tuned filter.

By comparing the waveforms in Figure 7 it can be observed that by increasing f_{sw} to the resonant minimum of each case the voltage total harmonic distortion (VTHD) falls significantly. In the first case the VTHD goes from 99.64% at 2500Hz to 13.25% at 6000Hz (Figure 7a). In the second case the VTHD goes from 7.11% at 2500Hz to 2.58% at 7000Hz (Figure 7b) and in the third case the VTHD goes from 3.46% at 2500Hz to 2.53% at 7000Hz (Figure 7c). The VTHD is not always reducing as the f_{sw} is increasing. More results can be seen in Table 3.

The conclusion from the above observations are that by studying the V_{GAIN} graph we are able to predict the optimum controller f_{sw} for a system with or without filters. Minimum harmonics are generated when the generator controller f_{sw} is at the resonant minimum of each case. In addition, the V_{GAIN} graph depicts the resonant peaks. The frequencies associated with resonant peaks must be avoided in order to keep voltage harmonics and overvoltages within limits.

However, in most cases the choice over the f_{sw} of the system is not possible at this wide scale and therefore the use of filters is needed. The analysis presented here can be useful to avoid resonant peaks, shift operating frequencies closer to resonant minimums and test filter types and parameters so that harmonics and over-voltages are mitigated.

Table 3 VTHD results from the simulation of the modelled TCCS for different filter cases and different controller switching frequencies

Switching Frequency (Hz)	No Filter	*LV LCR*	*LV LCR* and single tuned
1500	-	45.74%	31.29%
2500	99.64%	7.11%	3.46%
3000	67.81%	5.19%	4.21%
6000	13.25%	2.68%	2.61%
7000	15.25%	2.58%	2.53%
8500	19.35%	13.52%	12.72%

3.2.2 The effect of a LV LCR filter and a single tuned filter on the harmonics of the generator voltage

In this section, the distribution of harmonics at a specific frequency range will be depicted. In addition, the V_{GAIN} graphs shown in Figure 6 will be correlated with the distribution of harmonics in each case. For the simulation results we assume that the generator controller switching frequency is 2500Hz for all cases. Based

on the observations of the above section we expect to have higher harmonic components at resonant peaks and lower harmonic components at resonant minimums. Figure 8 compares the V_{GAIN} graph for the three different cases studied and the allocation of the voltage harmonics at the generator terminals.

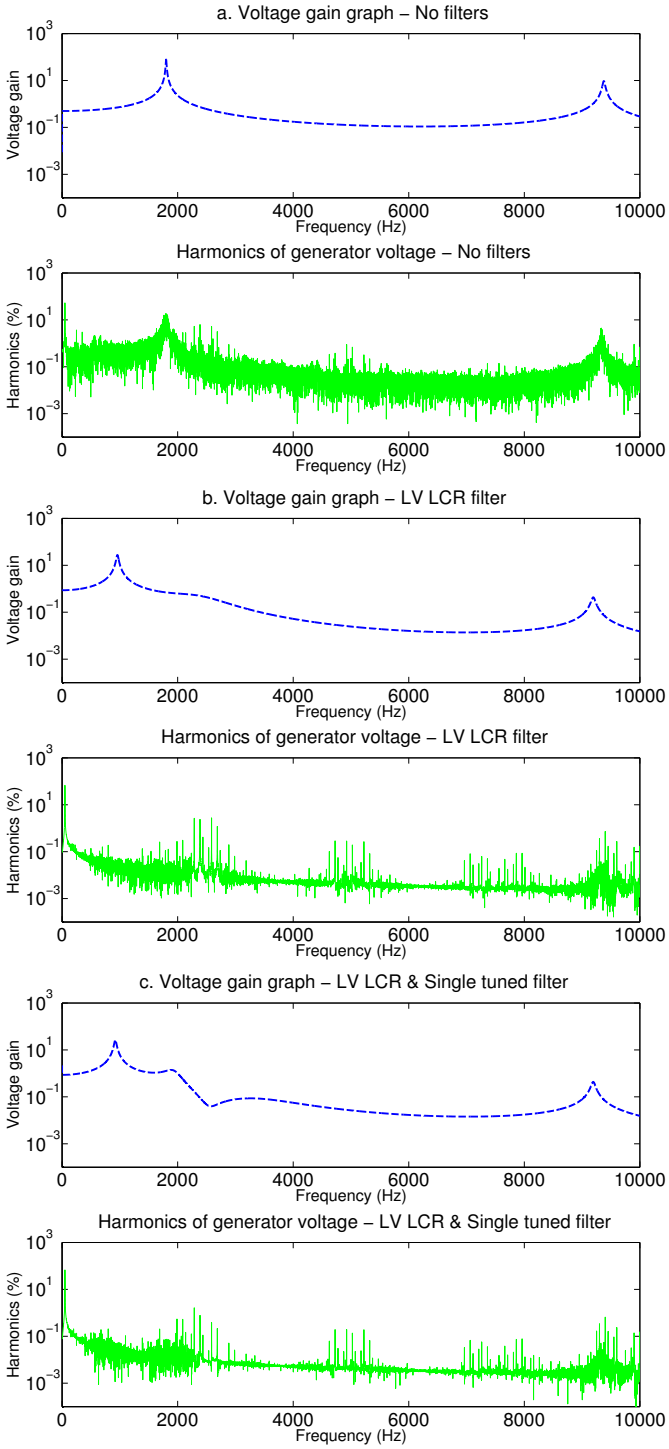

Figure 8. Comparison of the voltage gain graph and allocation of harmonics at the generator terminals. a. No filter b. LV LCR filter c. LV LCR filter and a single tuned filter at 2500Hz.

In Figure 8 the voltage gain graph for each case and the allocation of voltage harmonics at the generator terminals can be seen when the system is at rated operation and the generator controller f_{sw} is $2500Hz$. In both graphs, the voltage gain and the harmonic graph for each case y-axis is plotted in logarithmic scale while x-axis is plotted linearly. The harmonics graph shows the magnitude of harmonics in percentage of the fundamental.

The first observation is that there is a correlation between resonant peaks and appearance of high harmonics. This is evident in all three cases shown in Figure 8. For example, in Figure 8a the resonant peaks, based on the voltage gain graph, are at $1800Hz$ and $9350Hz$. Observing the harmonics graph it is shown that the percentage of harmonics around these frequencies are significant surpassing 10% per frequency. Similar results are presented in Figures 8b and 8c where harmonics appear around the resonant peaks of $800Hz$ and $9000Hz$. These harmonics will be referred as resonant harmonics.

The second observation from Figure 8 is the distribution of the characteristic harmonics generated by the generator controller. Based on the theory the characteristic harmonics from the generator controller appear at multiples of the fundamental frequency, 50Hz, around the multiples of the generator controller f_{sw}, 2500Hz. These characteristic harmonics are more visible in Figure 8b and 8c due to the significantly lower resonant harmonics. Comparing Figure 8b and Figure 8c it is observed that the characteristic harmonics around 2500Hz in Figure 8c are significantly lower. This is due to the installation of a single tuned filter at 2500Hz. This filter mitigates successfully the characteristic harmonics reducing the overall VTHD.

By describing Figure 8 we can conclude that the role of the *LV LCR* filter is to reduce voltage gain magnitude at all frequencies and consequently reduce the magnitude of resonant harmonics. The additional installation of a single tuned filter tuned at the generator controller f_{sw} reduces the characteristic harmonics achieving a desirable low distortion at the voltage terminals.

4 Conclusion

In this research paper an alternative way of integrating TCCS using long distance controls was proposed. The analysis focused on the frequency domain of the system since system resonance and voltage wave reflections can create high harmonic components flowing in the cables which lead to over-voltages at the generator terminals. From the results acquired it was concluded that a filter at the terminals of the VSC is required for a system with long distance controls. A *LV LCR* filter was designed and modelled based on literature. An additional contribution of this paper is the introduction of a single tuned filter in order to mitigate characteristic

harmonics generated by the generator controller. In order to study all the different cases voltage gain graphs were introduced and explained in detail. By knowing the resonant frequencies the controller operating frequencies can be shifted to resonant minimum frequencies and therefore reduce the harmonics affecting the system. This effect was demonstrated by comparing generator voltage waveforms at different generator controller switching frequencies. Moreover, research focused on the way in which the voltage gain graph changes when *LV LCR* filter and the single tuned filter were added. Finally, in this paper the allocation of harmonics of the generator voltage is studies and these harmonics are correlated with the voltage gain graphs. The electrical configuration proposed in this research paper can be used in any type of system where the generator is inaccessible and the power electronics have to be maintained regularly. Future research will focus on the detailed filter design and the parameter variations of the long cables.

Acknowledgements

The authors would like to thank ANDRITZ Hydro Hammerfest and The University of Edinburgh for funding this project.

References

[1] Department of Energy and Climate Change, 'UK ENERGY IN BRIEF 2014' (A National Statistics Publication, 2014). Available at https://www.gov.uk/government/statistics/uk-energy-in-brief-2014

[2] The Crown Estate., 'UK Wave and Tidal Key Resource Areas Project Summary Report: Version 2' (The Crown Estate, 2012). Available: http://www.thecrownestate.co.uk/energy-and-infrastructure/wave-and-tidal/publications/

[3] Krohn, D., Woods, M., Adams, J., Valpy, B., Jones, F., and Gardner, P.: 'Wave and Tidal Energy in the UK: Conquering Challenges, Generating Growth', renewableUK. Document Version: Issue 2, February 2013

[4] Spinato, F., Tavner, P.J., van Bussel, G.J.W., Koutoulakos, E.: 'Reliability of wind turbine subassemblies', *Renewable Power Generation, IET*, vol.3, no.4, pp.387-401, December 2009

[5] Von Jouanne, A, Rendusara, D.A, Enjeti, P.N., Gray, J.W.: 'Filtering techniques to minimize the effect of long motor leads on PWM inverter-fed AC motor drive systems', *Industry Applications, IEEE Transactions on* , vol.32, no.4, pp.919-926, Jul/Aug 1996

[6] Abdelsalam, AK., Masoud, M.I., Finney, S.J., Williams, B.W.: 'Vector control PWM-VSI induction motor drive with a long motor feeder: performance analysis of line filter networks', *Electric Power Applications, IET* , vol.5, no.5, pp.443-456, May 2011

[7] Tallam, R.M., Skibinski, G.L., Shudarek, T.A., Lukaszewski, R.A.: 'Integrated Differential-Mode and Common-Mode Filter to Mitigate the Effects of Long Motor Leads on AC Drives', *Industry Applications, IEEE Transactions on* , vol.47, no.5, pp.2075-2083, Sept.-Oct. 2011

[8] Xiaodong Liang, Faried, S.O., Ilochonwu, O.: 'Subsea Cable Applications in Electrical Submersible Pump Systems', *Industry Applications, IEEE Transactions on* , vol.46, no.2, pp.575-583, March-April 2010

[9] de Lima, AC.S., Dommel, H.W., Stephan, R.M.: 'Modeling adjustable-speed drives with long feeders', *Industrial Electronics, IEEE Transactions on* , vol.47, no.3, pp.549-556, Jun 2000

[10] Kuschke, M., Strunz, K.: 'Transient Cable Overvoltage Calculation and Filter Design: Application to Onshore Converter Station for Hydrokinetic Energy Harvesting', *Power Delivery, IEEE Transactions on*, vol.28, no.3, pp.1322-1329, July 2013

[11] J. Rodriguez, J. Pontt, C. Silva, R. Musalem, P. Newman, R. Vargas, and S. Fuentes, "Resonances and overvoltages in a medium-voltage fan motor drive with long cables in an underground mine," IEEE Trans. Ind. Appl., vol. 42, no. 3, pp. 856–863, May/Jun. 2006.

[12] Sousounis, M.; Shek, J.; Mueller, M., "Filter Design for Cable Overvoltage and Power Loss Minimization in a Tidal Energy System With Onshore Converters," *Sustainable Energy, IEEE Transactions on* , vol.PP, no.99, pp.1,9

[13] Whitby, B., Ugalde-Loo, C.E.: 'Performance of Pitch and Stall Regulated Tidal Stream Turbines', *Sustainable Energy, IEEE Transactions on*, vol.5, no.1, pp.64-72, Jan. 2014

[14] Zhibin Zhou, Scuiller, F., Charpentier, J.F., El Hachemi Benbouzid, M., Tianhao Tang: 'Power Smoothing Control in a Grid-Connected Marine Current Turbine System for Compensating Swell Effect', *Sustainable Energy, IEEE Transactions on*, vol.4, no.3, pp.816-826, July 2013

[15] Benelghali, S., El Hachemi Benbouzid, M., Charpentier, J.F., Ahmed-Ali, T., Munteanu, I.: 'Experimental Validation of a Marine Current Turbine Simulator: Application to a Permanent Magnet Synchronous Generator-Based System Second-Order Sliding Mode Control', *Industrial Electronics, IEEE Transactions on*, vol.58, no.1, pp.118-126, Jan. 2011

[16] Mekri, F., Ben Elghali, S., Benbouzid, M.E.H.: 'Fault-Tolerant Control Performance Comparison of Three- and Five-Phase PMSG for Marine Current Turbine Applications', *Sustainable Energy, IEEE Transactions on*, vol.4, no.2, pp.425-433, April 2013

[17] Ben Elghali, S.E., El Hachemi Benbouzid, M., Ahmed-Ali, T., Charpentier, J.-F.: 'High-Order Sliding Mode Control of a Marine Current Turbine Driven Doubly-Fed Induction Generator', *Oceanic Engineering, IEEE Journal of*, vol.35, no.2, pp.402-411, April 2010

[18] Sousounis, M.C., Shek, J.K.H., Mueller, M.A.: 'Modelling and control of tidal energy conversion systems with long distance converters'. *Power Electronics, Machines and Drives (PEMD 2014), 7th IET International Conference on*, Manchester, UK, 8-10 April 2014, pp.1-6

[19] Ben Elghali, S.E., Benbouzid, M.E.H., Charpentier, J.-F.: 'Modelling and control of a marine current turbine-driven doubly fed induction generator', *Renewable Power Generation, IET*, vol.4, no.1, pp.1-11, January 2010

[20] Takahashi, I., Noguchi, T.: 'A New Quick-Response and High-Efficiency Control Strategy of an Induction Motor', *Industry Applications, IEEE Transactions on*, vol.IA-22, no.5, pp.820-827, Sept. 1986

[21] Xue, Y., Xu, X., Habetler, T.G., Divan, D.M.: 'A low cost stator flux oriented voltage source variable speed drive', *Industry Applications Society Annual Meeting, 1990., Conference Record of the 1990 IEEE*, pp.410-415 vol.1, 7-12 Oct. 1990

[22] Wu, B., Lang, Y., Zargari, N. and Kouro, S.: 'Power Converters in Wind Energy Conversion Systems', in 'Power Conversion and Control of Wind Energy Systems', Hoboken, New Jersey: John Wiley & Sons, Inc. 2011, ch. 4. pp. 87 – 152.

[23] 'EMEC subsea cable', Available at: http://www.emec.org.uk/facilities/sub-sea-cables/ , Accessed on the 3rd of March 2015.

[24] S. Demmig, J. Andrews, and R.-D. Klug, "Control of subsea motors on multi-km cable lengths by Variable Frequency Drives," *Pet. Chem. Ind. Conf. Eur. Electr. Instrum. Appl.*, pp. 1–10, 2011.

Appendix

Table 4 Generator Parameters

Quantity	Value
Nominal Voltage (*V*)	6600
Apparent power range (*MVA*)	1.2 – 1.8

Frequency (Hz)	50
Stator resistance (pu)	0.00548
Stator inductance (pu)	0.08716
Rotor resistance (pu)	0.00399
Rotor inductance (pu)	0.08915
Mutual Inductance (pu)	3.99779
Rotor inertia ($kg.m^2$)	90
Pole pairs	3

Table 5 Transformer Parameters

Quantity	Value
Low Voltage Wye (V)	690
Medium Voltage Delta (V)	6600
Nominal frequency (Hz)	50
Wye resistance (pu)	0.0016
Wye inductance (pu)	0.0639
Delta resistance (pu)	0.0072
Delta inductance (pu)	0.0479
Magnetisation resistance (pu)	618
Magnetisation inductance (pu)	418